JOURNAL OF GUIDANCE, CONTROL, AND DYNAMICS
Vol. 16, No. 5, September–October 1993

# Application of Structured Singular Value Synthesis to a Fighter Aircraft

Andrew Sparks and Siva S. Banda
*Wright Laboratory, Wright-Patterson Air Force Base, Ohio 45433*

**The results of a design study to examine the control of a fighter aircraft at high angles of attack are presented. The flight condition considered represents an extreme point along a demanding, large angle maneuver. The control objective is to attain acceptable flying qualities despite variations and uncertainty in the aircraft's aerodynamic coefficients. Control laws are developed for a linear model of the aircraft using structured singular value synthesis to take the parameter uncertainty structure into account. Desired flying qualities are embedded in ideal models of the angle of attack, sideslip angle, and stability axis roll rate responses to pilot inputs. The control objective is met by minimizing the weighted error between the ideal model outputs and the plant outputs and including structured parameter uncertainty in the design model. Analysis of the closed-loop system assuming interdependent parameter variations is done to evaluate conservativeness. Low-order optimal Hankel norm approximations of balanced realizations of the control laws are found that maintain the performance and robustness characteristics of the full-order controllers.**

## I. Introduction

THE ability of a pilot to maneuver a fighter aircraft to advantage over an adversary will continue to be a decisive factor in future air combat. Increased maneuverability comes about through increased instantaneous and sustained turn rate capabilities. Both are dependent on the ability of the aircraft to fly at high angles of attack. At high angles of attack, where precise control of the aircraft motion is most crucial and the aerodynamics of the aircraft are most malevolent, the conventional control effectors are least effective. Hence, in the design of future fighter aircraft, unconventional control effectors such as thrust vectoring will be required in addition to the traditional aerodynamic effectors to provide safe, controlled flight.

The control system will play a key role in the development of fighter aircraft that will fly at high angles of attack, both in providing stability at the extreme conditions and by furnishing the pilot with good flying qualities throughout the maneuver. Control system design for these fighters is a challenging problem for several reasons. There are high levels of kinematic and inertial coupling at high angles of attack. The dynamics of the vehicle are inherently nonlinear, and linear approximations of the dynamics must be used judiciously. Most importantly, there are large amounts of uncertainty in the models used for control system design at the extreme operating conditions. This comes both from the fact that the models are highly nonlinear and from the lack of accurate data for these extreme operating points. A realistic design must meet the performance requirements for a specified level of uncertainty without being conservative. Control laws that meet performance requirements for unrealistic levels of uncertainty will sacrifice performance when used with the real system. The issue of meeting performance objectives for specific plant uncertainties will be addressed in this paper.

Recently, a multivariable control system design was performed on a model of a fighter aircraft.[1] The aircraft model

**Andrew Sparks graduated with a B.S. and an M.S. in Mechanical Engineering from Massachusetts Institute of Technology in 1986 and 1988, respectively. From February 1988 to August 1992 he worked as a Stability and Control Engineer in the Flight Controls Division of the Wright Laboratory. He is currently working on his Ph.D. at the University of Michigan in the Department of Aerospace Engineering. He is expected to return to the Wright Laboratory in 1995. His research interests include robust control theory and its application to aircraft. He is a Member of AIAA.**

**Siva S. Banda is an Aerospace Engineer at Wright Laboratory, Wright-Patterson Air Force Base, Ohio. His responsibilities include transitioning basic research results in the area of control theory to the aerospace industry. He has authored or coauthored more than 75 publications in the areas of multivariable control theory and application. He has received numerous awards from the U.S. Air Force for scientific achievement, including the Air Force Chief of Staff award from the Pentagon. He has served as a member of the AIAA Guidance, Navigation, and Control Technical Committee; on the Board of Directors of the American Automatic Control Council; as Chairman of the AIAA Awards Committee; and as Associate Editor of *Journal of Guidance, Control, and Dynamics*. He has been an Adjunct Associate Professor at Wright State University and at the University of Dayton. He is a Fellow of Wright Laboratory and is an Associate Fellow of AIAA.**

Received March 6, 1992; revision received Oct. 12, 1992; accepted for publication Oct. 22, 1992. 

included thrust vectoring nozzles to provide control power at high angle-of-attack, low dynamic pressure conditions where aerodynamic surfaces are ineffective. A linearized model of the aircraft at an extreme operating point along a high angle-of-attack maneuver trajectory was used in the design process. $H_\infty$ synthesis was used to minimize a weighted mixed sensitivity function at the output of the linear model. Performance requirements were met through frequency dependent weights on the output sensitivity and complementary sensitivity functions. Three other linearized points along the trajectory were used to assess the robustness of the controller to uncertainty and changes in the dynamics.

The $H_\infty$ control law design technique is very sensitive to structured parameter uncertainty.[2] The linear aircraft models describing different points along the maneuver[1] encompass a wide variation in dynamic pressure, and therefore have large parametric variations between them. This problem was overcome by an inner loop linear quadratic regulator (LQR) for the nominal design model that reduces the relative error between it and the linear models at the off design conditions. The $H_\infty$ synthesis technique was then applied to the nominal model with the LQR inner feedback loop closed. A fixed $H_\infty$ controller was found that provides robust stability for all of the linear points throughout the maneuver. Gain scheduling was addressed through a control selector that redistributes control commands to available effectors, i.e., aerodynamic surfaces at normal operating conditions and thrust vectoring at extreme conditions.

The results of the aforementioned study are highly encouraging. This paper illustrates a control design study for the same aircraft model using structured singular value (SSV) synthesis, or $\mu$-synthesis. The advantage of this approach is a quantitative accounting of the tradeoffs between the achievable level of performance and the robustness to a specific, structured uncertainty model. This accounting reduces the conservatism of the design. The issues of meeting specific performance and robustness requirements are addressed. This paper shows how the flight control design problem can be formulated within the $\mu$-synthesis framework to attain acceptable flying qualities and how robustness to specific uncertainties in aerodynamic coefficients can be accomplished.

## II. Problem Description

One of the design goals for the fighter aircraft is to develop control laws that will allow the pilot to perform a large angle, demanding maneuver. The purpose of this maneuver is to turn the aircraft toward an adversary after an unsuccessful first pass where both parties survive. The maneuver is important because it allows the pilot to launch a weapon before his opponent can. The maneuver is performed by pitching up to maximum angle of attack, increasing flight path angle, and decreasing airspeed. Then, at a critical point, the pilot rolls the aircraft about its velocity vector to change the heading by 180 deg. This maneuver is particularly challenging from a control design point of view, as it involves large variations in angle of attack and dynamic pressure, high rotational rates, large accelerations, and a large change in velocity.

This paper shows a point design for the fighter aircraft model. The design flight condition represents a point along the maneuver trajectory during the pitch up to maximum angle of attack, before the stability axis roll is executed. The speed at this condition is Mach 0.18, and the altitude is 10,000 ft. The angle of attack is approximately 70 deg, and the dynamic pressure is 33.6 lb/ft$^2$. At this low dynamic pressure condition, conventional control surfaces are ineffective. The thrust vectoring nozzles must be used for control. The design goal for the problem shown in this paper is to get acceptable flying qualities despite uncertainty in the aerodynamic coefficients.

For a flight control system to be acceptable, it must meet flying qualities requirements, so that the response of the aircraft to pilot commands is predictable and desirable. The flying qualities requirements are given in the military specification.[3] These requirements are modified somewhat to account for the extreme condition of the design point. Since the flight condition is at a high angle of attack, the short period frequency and damping requirements are stated in terms of the second-order equivalent system from pilot stick command to angle of attack. The dynamics such as the phugoid mode in the longitudinal dynamics and the spiral mode in the lateral directional dynamics are not of interest, since the design point is a transient condition and these modes will not contribute significantly to the response.

The short period frequency requirement is normalized by load factor per unit angle of attack. The square of the required short period frequency normalized by load factor per unit angle of attack must lie between 0.28 and 3.60. The short period damping must be greater than 0.35 and less than 1.3. The Dutch roll frequency and damping requirements are given in terms of the second-order equivalent system from rudder pedal input to sideslip angle, and the roll mode time constant is given in terms of the first-order equivalent system from pilot stick input to stability axis roll rate. The Dutch roll frequency must be higher than 1 rad/s, and the Dutch roll damping must be greater than 0.4 for the task described here. The equivalent roll mode time constant must be less than 1 s.

The flight control specification gives robustness measures in terms of gain and phase margins. These metrics are not well defined for multivariable systems, and generalizations to multivariable gain and phase margins may be conservative. For this paper, robustness to structured uncertainty in the aerodynamic parameters will be treated directly in the design process. Insufficient robustness will manifest itself in an unsuccessful design, and since the specific structure of the uncertainty is considered, will reflect inherent limitations in the nominal plant model.

## III. Model Description

A high fidelity nonlinear model of the fighter aircraft has been developed. The model is implemented in a generic nonlinear simulation package using a series of FORTRAN subroutines to describe the equations of motion, the aerodynamics, the engine, the actuators, and the sensors. The aerodynamic database encompasses a large range of dynamic pressures, angles of attack, and sideslip angles. The propulsion model includes a high performance variable geometry inlet and a thrust vectoring and reversing nozzle. Detailed sensor and actuator models with rate and position limits are also included.

The nonlinear model is linearized by using a small perturbation technique. The full-order nonlinear model consists of aerodynamic states, structural dynamics, actuator dynamics, and engine and nozzle dynamics. To get a linear model suitable for control law design, the high-order model was reduced to a conventional tenth-order aircraft model with five longitudinal and five lateral directional states. The trajectory related states of pitch angle, roll angle, heading angle, altitude, and airspeed were truncated to get a fifth-order model. The longitudinal model is given by

$$\begin{aligned} \dot{\alpha} &= Z_\alpha \alpha + q + Z_{\delta_{PV}} \delta_{PV} \\ \dot{q} &= M_\alpha \alpha + M_q q + M_{\delta_{PV}} \delta_{PV} \\ n_z &= (V/g)(\dot{\alpha} - q) \end{aligned} \tag{1}$$

where $\alpha$ is the angle of attack, $q$ is the pitch rate, $\delta_{PV}$ is the pitch vectoring nozzle deflection, $n_z$ is the normal acceleration, and $V$ is the airspeed. Outputs of the longitudinal model are

angle of attack, pitch angle, and normal acceleration. The lateral directional model is given by

$$\dot{\beta} = Y_\beta \beta + \frac{W_o}{V} p - r + Y_{\delta_{RV}} \delta_{RV} + Y_{\delta_{YV}} \delta_{YV}$$

$$\dot{p} = L_\beta \beta + L_p p + L_r r + L_{\delta_{RV}} \delta_{RV} + L_{\delta_{YV}} \delta_{YV}$$

$$\dot{r} = N_\beta \beta + N_p p + N_r r + N_{\delta_{RV}} \delta_{RV} + N_{\delta_{YV}} \delta_{YV} \tag{2}$$

$$\dot{\mu} = p \cos \alpha + r \sin \alpha$$

$$n_y = (V/g)(\dot{\beta} + r)$$

where $\beta$ is the sideslip angle, $p$ is the body axis roll rate, $r$ is the body axis yaw rate, $\dot{\mu}$ is the stability axis roll rate, $\delta_{RV}$ is the roll vectoring nozzle deflection, $\delta_{YV}$ is the yaw vectoring nozzle deflection, $W_o$ is the vertical velocity, and $n_y$ is the lateral acceleration. Outputs of the lateral directional model are sideslip angle, body axis roll and yaw rates, and lateral acceleration. The linear models at the nominal design point are given in the Appendix.

The actuator models for the thrust vectoring dynamics consist of second-order transfer functions with a natural frequency of 20 rad/s and a damping of 0.6. Rate limits of 60 deg/s and position limits of 30 deg are included in the nonlinear actuator models. The sensors include gyroscopes to produce measurement of pitch, roll, and yaw rates in the body axis and accelerometers to produce measurements of normal and lateral acceleration in the body axis. Angle-of-attack and sideslip feedback signals are constructed by augmenting the vane measurements from the air data unit with inertial data. All sensor measurements are assumed to be perfect, since the bandwidth of the sensors is well beyond that of the control system.

## IV. Structured Singular Value Synthesis

One of the most important advances in the past decade in the field of multivariable control is the development of $H_\infty$ control theory. Consider the plant given by the equations

$$\dot{x} = Ax + B_1 w + B_2 u$$

$$z = C_1 x + D_{11} w + D_{12} u \tag{3}$$

$$y = C_2 x + D_{21} w + C_{22} u$$

where $x$ is the state vector, $u$ is the input vector, $y$ is the output vector, $w$ is an exogenous input vector, and $z$ is an exogenous output vector. The well-known state-space $H_\infty$ theory[4] gives the equations to produce a stabilizing feedback controller from output vector $y$ to input vector $u$ that minimizes the induced $H_\infty$ norm between $w$ and $z$.

The plant must meet the following assumptions: $(A, B_2)$ must be stabilizable, $(A, C_2)$ must be detectable, $D_{12}$ and $D_{21}$ must have full rank,

$$\begin{bmatrix} A - j\omega I & B_2 \\ C_1 & D_{12} \end{bmatrix}$$

must have full column rank for all $\omega$, and

$$\begin{bmatrix} A - j\omega I & B_1 \\ C_2 & D_{21} \end{bmatrix}$$

must have full row rank for all $\omega$. The column and row rank conditions of these two matrices are to assure that the transfer matrices from $w$ to $y$ and from $u$ to $z$ have no invariant zeros on the imaginary axis. Also assume for convenience that $D_{11}$ and $D_{22}$ are zero, and that the system is scaled so that

$$D_{12}^T [C_1 \quad D_{12}] = [0 \quad I] \qquad \begin{bmatrix} B_1 \\ D_{21} \end{bmatrix} D_{21}^T = \begin{bmatrix} 0 \\ I \end{bmatrix}$$

These last assumptions are made only to simplify the solution, and can be easily removed. The plant can be manipulated to transform an arbitrary plant to one that meets these conditions.[5] Define two Hamiltonian matrices and two Riccati equations

$$H_\infty = \begin{bmatrix} A & \gamma^{-2} B_1 B_1^T - B_2 B_2^T \\ -C_1^T C_1 & -A^T \end{bmatrix}$$

$$J_\infty = \begin{bmatrix} A^T & \gamma^{-2} C_1^T C_1 - C_2^T C_2 \\ B_1 B_1^T & -A \end{bmatrix} \tag{4}$$

$$A^T X_\infty + X_\infty A + X_\infty (\gamma^{-2} B_1 B_1^T - B_2 B_2^T) X_\infty + C_1^T C_1 = 0 \tag{5}$$

$$A Y_\infty + Y_\infty A^T + Y_\infty (\gamma^{-2} C_1^T C_1 - C_2^T C_2) Y_\infty + B_1 B_1^T = 0 \tag{6}$$

Under the conditions that the Hamiltonian matrices $H_\infty$ and $J_\infty$ do not have any poles on the imaginary axis, $X_\infty$ and $Y_\infty$ are positive semidefinite solutions to the two Riccati equations, and the spectral radius of the product of the Riccati solutions, $\rho(X_\infty Y_\infty)$ is less than $\gamma^2$, then the controller that constrains the $H_\infty$ norm between $w$ and $z$ of Eq. (3) to be less than $\gamma$ is given by

$$\dot{x}_\infty = A_\infty x_\infty - Z_\infty L_\infty y$$

$$u = F_\infty x_\infty \tag{7}$$

where

$$A_\infty = A + \gamma^{-2} B_1 B_1^T X_\infty + B_2 F_\infty + Z_\infty L_\infty C_2$$

$$F_\infty = -B_2^T X_\infty$$

$$L_\infty = -Y_\infty C_2^T \tag{8}$$

$$Z_\infty = (I - \gamma^{-2} Y_\infty X_\infty)^{-1}$$

An advantage of $H_\infty$ synthesis theory is its ability to treat model uncertainties in the form of complex perturbations to a nominal model. Consider the generalized plant $G$ and the uncertainty representation $\Delta$ of Fig. 1. The matrix $\Delta$ can be any complex matrix. The generalized plant consists of the nominal plant model, the controller, and weighting and scaling functions so that the complex uncertainty matrix has a maximum singular value of unity. The system can be partitioned as

$$G = \begin{bmatrix} G_{11} & G_{12} \\ G_{21} & G_{22} \end{bmatrix} \tag{9}$$

where $w_1$ and $z_1$ correspond to plant uncertainty and $w_2$ and $z_2$ correspond to performance variables. Robust stability is a measure of whether the closed-loop plant will go unstable for any perturbation $\Delta$. Assuming no particular structure of $\Delta$, the small gain theorem assures robust stability when

$$\|G_{11}\|_\infty \leq 1 \tag{10}$$

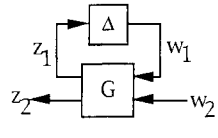


**Fig. 1 Generalized plant.**

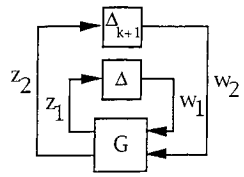


**Fig. 2 Plant with uncertainty and performance blocks.**

since the perturbation matrix $\Delta$ is scaled to be less than one. Thus, by constraining the $H_\infty$ norm between $w_1$ and $z_1$ to be less than one, robustness to all uncertainty $\Delta$ is guaranteed. In a similar fashion, frequency dependent weights are included in $G$ to weight the performance variables, so that nominal performance is assured when

$$\|G_{22}\|_\infty \leq 1 \tag{11}$$

Thus, by constraining the $H_\infty$ norm between $w_2$ and $z_2$ to be less than one, performance, as defined by the generalized plant $G$ including the weighting functions, is guaranteed.

When the model uncertainty becomes highly structured, then the $H_\infty$ theory is potentially conservative. The perturbation matrix $\Delta$ may not be an accurate representation of the true uncertainty, since it may overbound the true uncertainty and represent perturbations to the nominal plant that are unrealistic. It can be made less conservative by considering the particular structure of the uncertainty. Structured robust stability assumes that the perturbation block has a certain structure to it based on the uncertainty representation of the plant. A general model of the uncertainty is

$$\underline{\Delta} = \left\{\text{diag}(\delta_1,\delta_2,\ldots,\delta_m,\Delta_1,\Delta_2,\ldots,\Delta_n) \mid \delta_i \subset C,\ \Delta_j \subset C^{k\times k}\right\} \tag{12}$$

$$B\underline{\Delta} = \left\{\Delta \subset \underline{\Delta} \mid \bar{\sigma}(\Delta) \leq 1\right\} \tag{13}$$

where $\underline{\Delta}$ is the set of all possible perturbations and $B\underline{\Delta}$ is normalized to unity. The uncertainty model, then, consists of a diagonal matrix of scalar and full complex uncertainty blocks. The most general case, that is, unstructured uncertainty, is a subset of $\underline{\Delta}$ and would consist of a single full complex block.

The structured singular value is a measure of robustness to complex perturbations that have a given structure.[6,7] The structured singular value $\mu$ of a complex matrix $M$ is defined as the inverse of the maximum singular value of the smallest destabilizing perturbation that has the specified structure.

$$1/\mu(M) = \min_{\Delta \subset B\underline{\Delta}} \left[\bar{\sigma}(\Delta) \mid \det(I - M\Delta) = 0\right] \tag{14}$$

If the matrix $M$ is a transfer function matrix evaluated at some location $s_0$ in the complex plane, then the inverse of $\mu[M(s_0)]$ is the maximum singular value of the smallest perturbation $\Delta$ of the given structure that moves a complex pole to that location, since the zeros of $\det(I - M\Delta)$ are the poles of the perturbed system. Thus, if $M$ is a stable closed-loop transfer matrix, and $\mu(M)$ is evaluated along the imaginary axis, then $\mu(M)$ is a function of frequency that gives the size of the smallest allowable $\Delta$ that moves a closed-loop pole to the imaginary axis. Since the uncertainty representation is scaled to be less than one, if $\mu(M)$ is less than one over all frequencies, then the system is stable for all possible uncertainties in the allowed set. The maximum of $\mu$ over a frequency range is defined as

$$\|G\|_\mu = \sup_\omega \mu\left[G(j\omega)\right] \tag{15}$$

Structured robust stability is defined by

$$\|G_{11}\|_\mu \leq 1 \tag{16}$$

Robust performance is a measure of whether all of the performance requirements are met for the given uncertainty. The test for robust performance can be accomplished using the structured singular value, where the perturbation that represents the uncertainty now includes a full complex block, as shown in Fig. 2, to represent the performance

$$\tilde{\underline{\Delta}} = \left\{\tilde{\Delta} = \text{diag}(\Delta, \Delta_{k+1}) \mid \Delta \subset \underline{\Delta}\right\} \tag{17}$$

Structured robust performance is guaranteed when

$$\|G\|_\mu \leq 1 \tag{18}$$

Unfortunately, $\mu$ cannot be computed directly. Instead, upper and lower bounds on $\mu$ can be computed

$$\sup_U \rho(UM) \leq \mu(M) \leq \inf_D \bar{\sigma}(DMD^{-1}) \tag{19}$$

where $U$ is a unitary matrix whose structure is the same as that of the perturbation, and $D$ is a matrix whose structure depends on that of the perturbation structure.[7]

Robust performance for structured uncertainty can be met by combining $H_\infty$ control with analysis of the structured singular value for the uncertainty representation given in Eq. (17). An $H_\infty$ control law is generated for a plant assuming no structure to the uncertainty. The upper bound of $\mu$ of the closed-loop system is computed using Eq. (19) over a specified frequency range. Information about the structure of the uncertainty is used to restrict $D$ to have a certain structure. A rational approximation of the $D$ scaling is computed and used to scale the original plant, and a second $H_\infty$ control law is found for the scaled plant. Again, $\mu$ can be computed for the closed-loop system. This process is repeated until the structured singular value is less than one at all frequencies.

## V. Control Law Design

Separate control laws were found for the longitudinal and the lateral directional models. Robustness to parameter uncertainties was accomplished by modeling the uncertainties in the aerodynamic coefficients as perturbations of the nominal model. Actuator and sensor constraints were taken into consideration by including models of the actuator dynamics and sensor noise inputs and penalizing the transfer function between the two.

In each case, an ideal model of the desired dynamics was used in the control law formulation. The desired flying qualities are embedded in these ideal models. The ideal angle-of-attack model defines the desired short period natural frequency and damping. The ideal sideslip model defines the desired Dutch roll natural frequency and damping. The ideal stability axis roll rate model defines the roll mode time constant. For each case, a synthesis model was formed using nominal plant dynamics and the ideal model dynamics. The error between the two was penalized using a frequency dependent weight, and the norm of the transfer function between the pilot command and the weighted error was minimized.

### A. Longitudinal Design

A block diagram of the longitudinal synthesis model is shown in Fig. 3. The nominal plant model consists of second-order short period dynamics from Eq. (1). The input to the model is pitch thrust vectoring, and the outputs are angle of attack, pitch angle, and normal acceleration. The actuator model is a second-order transfer function with a natural frequency of 20 rad/s and damping of 0.6. The ideal model is a second-order transfer function whose natural frequency and

damping are chosen to be 3.0 rad/s and 0.7, the desired short period short frequency and damping.

The frequency dependent weight $W_p$ penalizes the difference between the angle of attack in the nominal model and the output of the ideal model. The weight is chosen to be the transfer function $0.1(s+30)/(s+0.03)$. This weight is selected to be large at low frequency and small at high frequency for good tracking of pilot commands. The weights on the states of the actuator model are included to penalize control activity. To keep the order of the controller as low as possible, the weights are chosen to be constant. The diagonal elements of the weighting matrix $W_a$ on the pitch vectoring actuator position, rate, and acceleration are 0.01, 0.05, and 0.1, respectively. Similarly, exogenous inputs are included on the outputs to represent sensor noise. The diagonal elements on the weighting matrix $W_n$ on the angle of attack, pitch rate, and normal acceleration noise are 0.05, 0.01, and 0.01, respectively.

The uncertainty in the model is due to the errors and variations in the aerodynamic coefficients. For the longitudinal case, it is assumed that the uncertain parameters are $M_\alpha$, $M_q$, and $M_{\delta_{PV}}$. Each parameter is assumed to be within 25% of its nominal value, so that each parameter consists of its nominal value plus an uncertainty modeled as a perturbation. These uncertainties are represented by scalar perturbations to the nominal model. A model with perturbations $\Delta$ can be formed as[8]

$$\begin{aligned} \dot{x} &= Ax + Bu + B_\Delta u_\Delta \\ y_\Delta &= C_\Delta x + D_\Delta u \\ y &= Cx \\ u_\Delta &= \Delta y_\Delta \end{aligned} \tag{20}$$

A diagonal perturbation matrix $\Delta$ whose elements vary between $-1$ and 1 is formed, and the matrices $B_\Delta$, $C_\Delta$, and $D_\Delta$ are formed using the assumed values of the parameter perturbations. The structure of the matrices account for the particular uncertain parameters, and the sizes of the nonzero elements account for the magnitudes of the uncertain parameters.

The longitudinal synthesis model has uncertainty inputs $u_\Delta$ and outputs $y_\Delta$, corresponding to the three uncertain parameters. There are two performance inputs $\alpha_{com}$ and $n$ and two

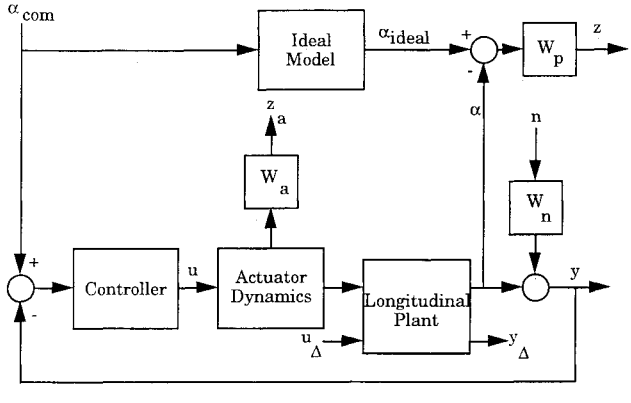


**Fig. 3 Longitudinal synthesis model.**

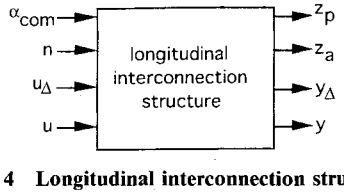


**Fig. 4 Longitudinal interconnection structure.**

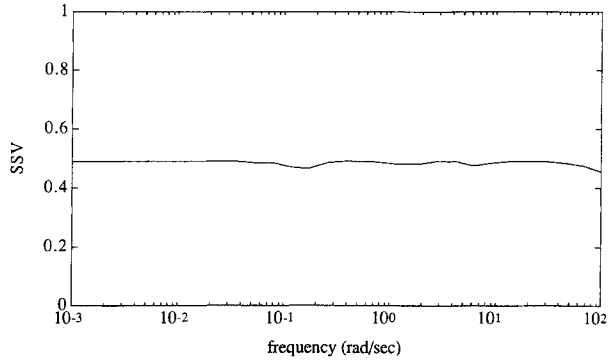


**Fig. 5 SSV of nominal longitudinal controller.**

performance outputs $z_p$ and $z_a$. The control input is $u$, and the measured output is $y$. The inputs and outputs of the synthesis model are rearranged to form the interconnection structure shown in Fig. 4, which is used in $H_\infty$ synthesis. The structure of the uncertainty block corresponds to this interconnection structure. The uncertainty is diagonal, with three scalar blocks corresponding to the parameter uncertainty, a scalar block corresponding to the angle-of-attack command and error, and a $3\times 3$ full block corresponding to the actuator outputs and sensor noise inputs. The $H_\infty$ control law minimizes the $H_\infty$ norm between all of the exogenous inputs $u_\Delta$, $\alpha_{com}$, and $n$ and all of the exogenous outputs $y_\Delta$, $z_p$, and $z_a$. Using $\mu$-synthesis to scale the plant using the $D$ scaling matrices from Eq. (19) will reduce conservatism by taking the structure of the uncertainty into account.

To begin, the $\mu$-synthesis design was completed without the parameter uncertainty in the design model. The inputs $u_\Delta$ and outputs $y_\Delta$ in the interconnection structure in Fig. 4, corresponding to the uncertain parameters in the state-space model, were truncated, and the $\mu$-synthesis design was carried out with the performance inputs and outputs only. This procedure was done to determine the limits of performance of the nominal plant model. When the parameter uncertainty is introduced into the problem, the nominal performance will be traded in exchange for robustness to uncertain parameters. The $\mu$-synthesis is carried out by finding an $H_\infty$ control law for the interconnection structure, and performing $\mu$-analysis on the closed-loop system. The uncertainty block consists of a scalar block for the command and a full block for the actuator and sensor inputs and outputs. The $D$ matrices from the upper bound computation in Eq. (19) are used to scale the interconnection structure, and the process is repeated. The $\mu$ plot of the nominal longitudinal control laws is shown in Fig. 5. The value of $\mu$ is well below one at all frequencies, and so the performance goal has been met for the nominal model.

To understand the importance of including the parameter uncertainty in the design model, $\mu$-analysis was performed on the closed-loop system. Now, the uncertainty inputs and outputs in the interconnection structure are included in the analysis. Two different models of the parameter uncertainty were used. First, the uncertain parameters were assumed to vary independently, so that the uncertainty structure was a diagonal matrix of independent scalars. Second, the parameters were assumed to vary together, so that the uncertainty structure was a diagonal matrix with repeated scalars. The plots of the structured singular values are shown in Fig. 6. The solid line is $\mu$ assuming independent parameter variations, and the dashed line is $\mu$ assuming dependent parameter variations. As expected, both controllers show poor robustness to the parameter uncertainties since they were not included in the design model. The robustness is worse for independent parameter perturbations, since this includes a larger set of uncertainties.

Finally, a $\mu$-synthesis controller was found for the interconnection structure shown in Fig. 4, including parameter perturbations. Now, the uncertainty structure includes inde-

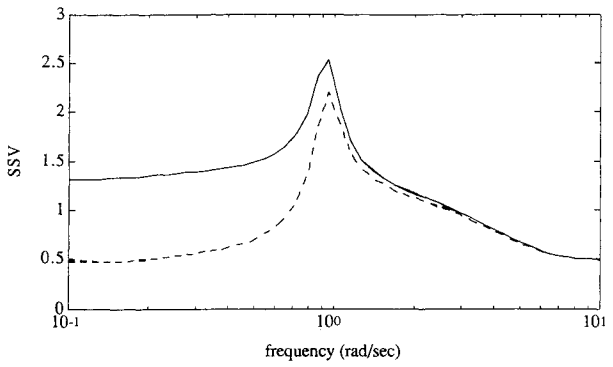


**Fig. 6 SSV with parameter uncertainty of nominal longitudinal controller.**

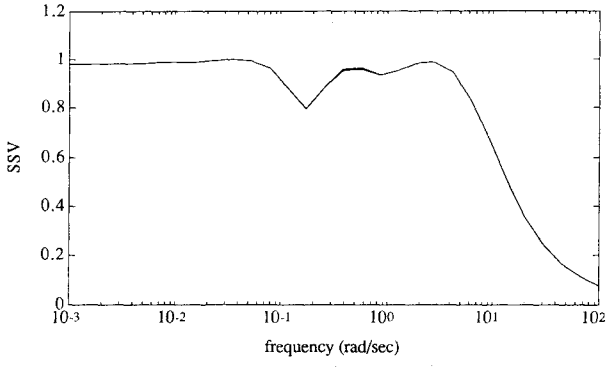


**Fig. 7 SSV of longitudinal controller with parameter robustness.**

pendent scalar blocks to represent the perturbations in the aerodynamic coefficients. After several iterations, the structured singular value converged. This is shown in Fig. 7. Since the structured singular value is less than one at all frequencies, the performance requirements are met, despite the parameter uncertainties.

### B. Lateral Directional Design

A block diagram of the lateral directional synthesis model is shown in Fig. 8. The nominal model includes third-order roll and Dutch roll dynamics from Eq. (2). The inputs to the model are roll and yaw thrust vectoring. Roll thrust vectoring is accomplished by differential pitch thrust vectoring. The outputs of the model are sideslip angle, roll and yaw rate, and lateral acceleration. The actuator models for both the roll and yaw thrust vectoring are second-order transfer functions with poles at 20 rad/s and damping of 0.6. The ideal model for the roll response is a first-order transfer function whose time constant is 0.6, the desired roll mode time constant. The ideal model for the sideslip response is a second-order transfer function whose natural frequency and damping are 3.0 and 0.7, the desired Dutch roll natural frequency and damping.

The frequency dependent weights $W_\beta$ and $W_\mu$ penalize the differences between the sideslip and the stability axis roll rate in the nominal model and the outputs of the ideal sideslip and roll models. The weights are chosen to be $0.1(s+30)/(s+0.03)$. The weights $W_a$ on the roll and yaw vectoring actuator positions, rate, and accelerations are 0.005, 0.025, and 0.05, respectively. The weights $W_n$ on the sideslip angle, roll and yaw rate, and lateral acceleration noise are 0.05, 0.01, 0.01, and 0.01, respectively. The stability axis roll rate command is broken into body axis roll and yaw rate commands, and the measured roll and yaw rates are combined in the synthesis model to generate the ideal model error.

The uncertainty in the model is due to the errors and variations in the aerodynamic coefficients. For the lateral case, it is assumed that the uncertain parameters are $L_\beta$, $N_\beta$, $L_{\delta_{RV}}$, and $N_{\delta_{YV}}$. Each parameter is assumed to be within 10% of its nominal value. The perturbations are rearranged as in the longitudinal case to obtain input and output vectors $u_\Delta$ and $y_\Delta$.

The lateral directional synthesis model has uncertainty inputs $u_\Delta$ and outputs $y_\Delta$ corresponding to the four uncertain parameters. There are three performance inputs, $\mu_{\text{com}}$, $\beta_{\text{com}}$, and $n$, and three performance outputs, $z_\mu$, $z_\beta$, and $z_a$. The control input is $u$, and the measured output is $y$. The inputs and outputs are rearranged to form an interconnection structure, shown in Fig. 9. The uncertainty block corresponding to this interconnection structure has four scalar elements corresponding to the parameter uncertainty, a $2\times 2$ full block corresponding to the commands and errors, and a $6\times 4$ full block corresponding to the actuator and sensor inputs and outputs.

Once again, the $\mu$-synthesis design was completed to determine the limits of performance for the nominal model. The inputs $u_\Delta$ and outputs $y_\Delta$ in the interconnection structure in Fig. 9 corresponding to the uncertain parameters in the state-space model were truncated, and the $\mu$-synthesis design was carried out with the performance inputs and outputs only. The structured singular value plot of the final iteration is shown in Fig. 10. As in the longitudinal case, it is well below one at all frequencies, and so the performance requirements are met for the nominal plant.

To see the robustness of this controller to parameter uncertainty, $\mu$-analysis was performed using the uncertainty inputs and outputs in the interconnection structure and the scalar uncertainty representation of the uncertain parameters. As in the longitudinal case, dependent and independent parameter perturbations were assumed. The plot of the structured singular values is shown in Fig. 11. The solid lines are $\mu$ for independent parameter variations, and the dashed lines are $\mu$ for dependent parameter variations. As expected, both controllers show poor robustness to the parameter uncertainties since they were not included in the design model.

The uncertainty inputs and outputs were included in the interconnection structure, and $\mu$-synthesis designs were performed for robust performance. A plot of the structured singular value of the closed-loop system is shown in Fig. 12. Now, as the parameter uncertainties have been included in the design model, the controllers show robust performance, since the

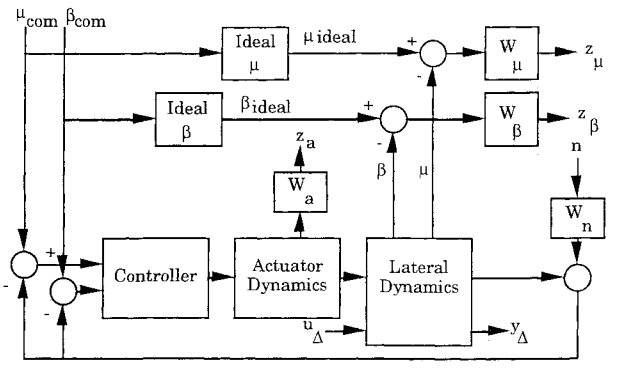


**Fig. 8 Lateral synthesis model.**

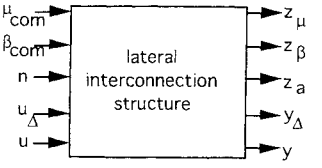


**Fig. 9 Lateral directional interconnection structure.**

plots are all below one. The two lines shown are the upper and lower bound computations.

## VI. Analysis of Control Laws

The closed-loop systems were formed using the $\mu$-synthesis controller with the nominal plant model. The nonlinear actuator models with rate and position limits were used to simulate realistic actuator constraints. The response of the closed-loop systems to step commands in angle of attack and stability axis roll rate were simulated, and results plotted in Figs. 13 and 14. In each case, the ideal model response is plotted along with the actual response. The ideal response is shown with the dashed line. Both controllers provide good command tracking at this flight condition and are very close to the ideal model response.

The parameters in the flight control design problem do not vary independently. In fact, they are all functions of dynamic pressure and angle of attack. Since they have a strong dependence on dynamic pressure, one representation of them is that they vary together. To evaluate the conservativeness of the controller to dependence of the uncertain parameters, a $\mu$-analysis of the controllers was performed by using the same block structure as in the synthesis, but by assuming dependent parameter uncertainty. Although this is a simplification of the parameter uncertainty description, it does show the effect of dependent parameter variations and provides a lower bound on the structured singular value.

The plots of the structured singular value for the two uncertainty models are shown in Figs. 15 and 16. The dashed lines are the $\mu$ plots for independent parameter variations, and the solid lines are the $\mu$ plots for independent variations. As expected, the structured singular value plots found by assuming dependent perturbations are below those found by assuming independent perturbations. The peak value of $\mu$ for the longitudinal controller is slightly less than one, and that for the lateral controller is about 0.9. Although the assumption that the parameters are independent is conservative, the results are very similar, and it is computationally simpler.

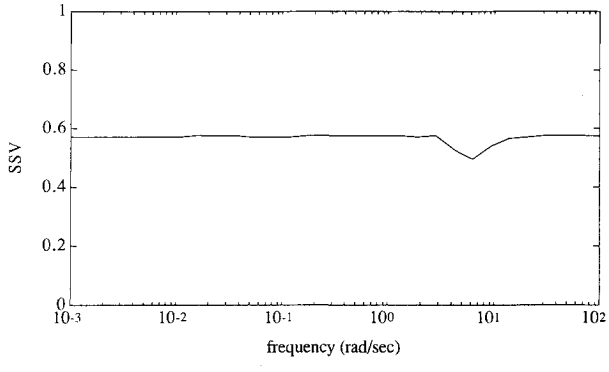


**Fig. 10 SSV of nominal lateral controller.**

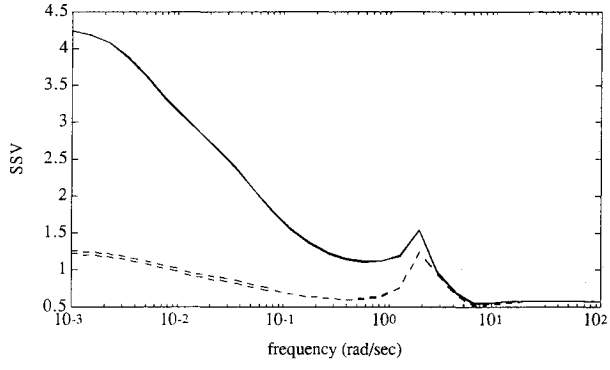


**Fig. 11 SSV with parameter uncertainty of nominal lateral controller.**

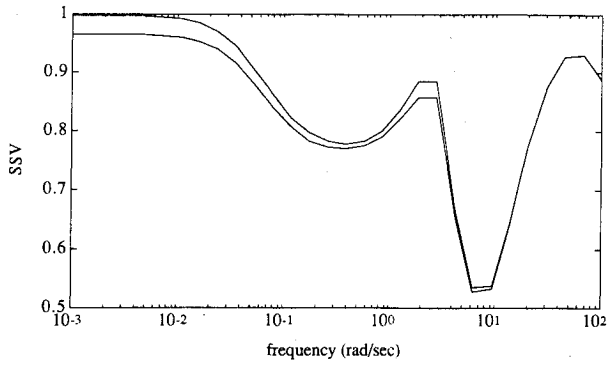


**Fig. 12 SSV of lateral controller with parameter robustness.**

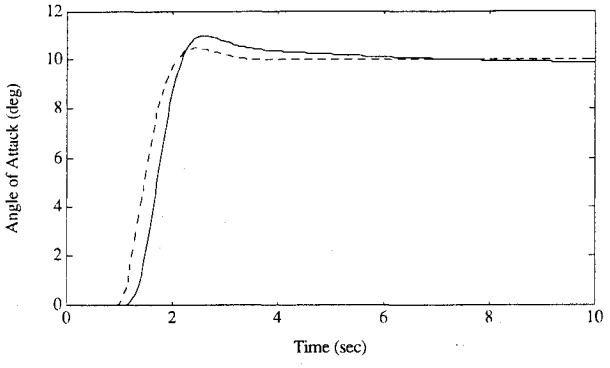


**Fig. 13 Angle-of-attack response.**

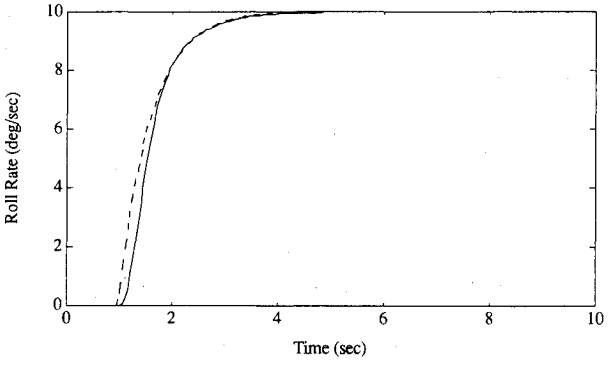


**Fig. 14 Roll rate response.**

## VII. Model Order Reduction

The $\mu$-synthesis controllers are very high order, since the order is equal to the sum of the plant model, the actuator model, the ideal model, the frequency dependent weights, and the rational function approximations of the diagonal scaling used. The full-order longitudinal controller has 19 states, and the full-order lateral directional controller has 24 states. The orders of the controllers must be reduced without degrading the performance and robustness characteristics.

In each case, a balanced realization of each of the controllers is produced. This result balances the observability and

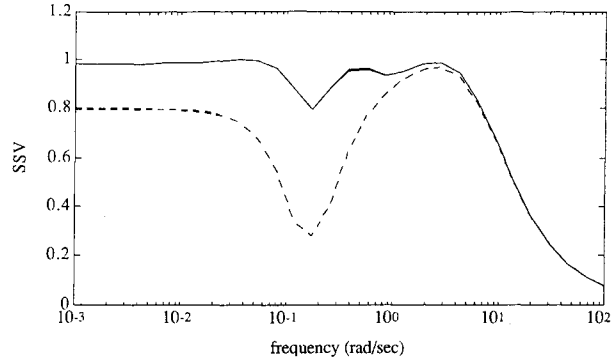


**Fig. 15 SSV of longitudinal controller with dependent and independent perturbations.**

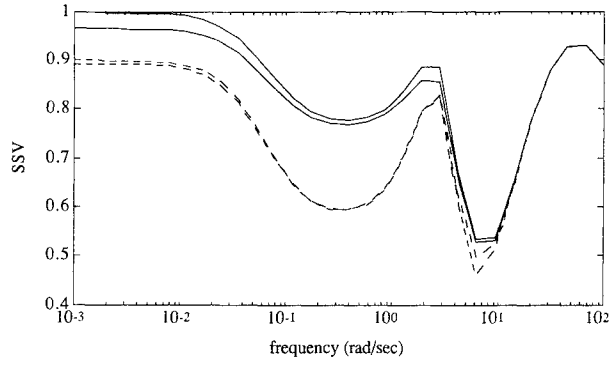


**Fig. 16 SSV of lateral controller with dependent and independent perturbations.**

controllability grammians. Then the model is reduced by computing the optimal Hankel norm approximation using the Hankel singular values as a guide on the maximum error between the full- and reduced-order controllers.[9] A $\mu$-analysis of the reduced-order controller is performed to ensure that the performance and robustness properties are preserved. The longitudinal controller was reduced to sixth-order without degrading $\mu$, and the lateral directional controller was reduced to twelfth-order without degrading $\mu$. Reducing either controller further resulted in controllers that did not meet robust performance.

## VIII. Conclusions

Control laws were designed for the longitudinal and lateral directional dynamics of a fighter aircraft using $\mu$-synthesis at a high angle-of-attack flight condition. Good flying qualities and robustness to uncertainties and variations in specific parameters were achieved. The conservativeness of assuming independent parameter perturbations was investigated. The resulting control laws were of very high order, and each was reduced to a more reasonable size by performing a balanced realization and taking the optimal Hankel norm approximation. The performance and robustness of the closed-loop system with the reduced-order controllers did not degrade from that of the full-order controllers.

## Appendix

Longitudinal model:

$$A = \begin{bmatrix} 0.0264 & 0.9905 \\ -0.8810 & -0.2079 \end{bmatrix} \quad B = \begin{bmatrix} -0.0520 \\ -4.3434 \end{bmatrix}$$

$$C = \begin{bmatrix} 1.0000 & 0.0000 \\ 0.0000 & 1.0000 \\ 0.1611 & 0.0000 \end{bmatrix} \quad D = \begin{bmatrix} 0.0000 \\ 0.0000 \\ -0.3174 \end{bmatrix}$$

Lateral directional model:

$$A = \begin{bmatrix} -0.0476 & 0.9407 & -0.3383 \\ -4.4641 & -0.5268 & 0.1245 \\ -0.3009 & 0.0069 & -0.0029 \end{bmatrix}$$

$$B = \begin{bmatrix} 0.0000 & 0.1224 \\ -1.3232 & 0.2674 \\ -0.0234 & -3.6664 \end{bmatrix}$$

$$C = \begin{bmatrix} 1.0000 & 0.0000 & 0.0000 \\ 0.0000 & 1.0000 & 0.0000 \\ 0.0000 & 0.0000 & 1.0000 \\ -0.2905 & 5.7415 & 0.0000 \end{bmatrix} \quad D = \begin{bmatrix} 0.0000 & 0.0000 \\ 0.0000 & 0.0000 \\ 0.0000 & 0.0000 \\ 0.0000 & 0.7471 \end{bmatrix}$$

## References

[1]Chiang, R. Y., Safonov, M. G., Madden, K. P., and Tekawy, J. A., "A Fixed $H^\infty$ Controller for a Supermaneuverable Fighter Aircraft Performing the Herbst Maneuver," *Proceedings of the 29th Conference on Decision and Control,* Inst. of Electrical and Electronics Engineers, Piscataway, NJ, 1990.

[2]Chiang, R. Y., Safonov, M. G., and Tekawy, J. A., "Robust Control Design with Large Parametric Robustness," *Proceedings of the 1990 American Control Conference,* Inst. of Electrical and Electronics Engineers, Piscataway, NJ, 1990.

[3]*Military Standard—Flying Qualities of Piloted Airplanes,* MIL-STD-1797A, Jan. 30, 1990.

[4]Doyle, J. C., Glover, K., Khargonekar, P., and Francis, B., "State Space Solutions to Standard $H_2$ and $H_\infty$ Control Problems," *IEEE Transactions on Automatic Control,* Vol. 34, Aug. 1989, pp. 18-36.

[5]Safonov, M. G., Limebeer, D. J., and Chiang, R. Y., "Simplifying the $H_\infty$ Theory via Loop Shifting, Matrix Pencil, and Descriptor Concepts," *International Journal of Control,* Vol. 50, No. 6, 1987, pp. 2467-2488.

[6]Doyle, J. C., "Analysis of Feedback Systems with Structured Uncertainties," *IEE Proceedings,* Vol. 129, Pt. D, No. 6.

[7]Doyle, J. C., "Structured Uncertainty in Control System Design," *Proceedings of the 24th Conference on Decision and Control,* Inst. of Electrical and Electronics Engineers, Piscataway, NJ, 1985.

[8]Steinbuch, M., Terlouw, J. C., and Bosgra, O. H., "Robustness Analysis for Real and Complex Perturbations Applied to an Electro-Mechanical System," *Proceedings of the 1991 American Control Conference,* Inst. of Electrical and Electronics Engineers, Piscataway, NJ, 1991.

[9]Glover, K., "All Optimal Hankel Norm Approximations of Linear Multivariable Systems and Their $L^\infty$-Error Bounds," *International Journal of Control,* Vol. 6, June 1984, pp. 1115-1193.

[10]Doyle, J. C., Lenz, K., and Packard, A., "Design Examples Using $\mu$-Synthesis: Space Shuttle Lateral Axis FCS During Reentry," *Proceedings of the 25th Conference on Decision and Control,* Inst. of Electrical and Electronics Engineers, Piscataway, NJ, 1986.